ARL-TR-7487 ● SEP 2015

US Army Research Laboratory

Large-Scale, Full-Wave Scattering Phenomenology Characterization of Realistic Trees: Preliminary Results

by DaHan Liao and Traian Dogaru

NOTICES

Disclaimers

ARL-TR-7487 ● SEP 2015

US Army Research Laboratory

Large-Scale, Full-Wave Scattering Phenomenology Characterization of Realistic Trees: Preliminary Results

by DaHan Liao and Traian Dogaru
Sensors and Electron Devices Directorate, ARL

REPORT DOCUMENTATION PAGE			*Form Approved* *OMB No. 0704-0188*
Public reporting burden for this collection of information is estimated to average 1 hour per response, including the time for reviewing instructions, searching existing data sources, gathering and maintaining the data needed, and completing and reviewing the collection information Send comments regarding this burden estimate or any other aspect of this collection of information, including suggestions for reducing the burden, to Department of Defense, Washington Headquarters Services, Directorate for Information Operations and Reports (0704-0188), 1215 Jefferson Davis Highway, Suite 1204, Arlington, VA 22202-4302 Respondents should be aware that notwithstanding any other provision of law, no person shall be subject to any penalty for failing to comply with a collection of information if it does not display a currently valid OMB control number **PLEASE DO NOT RETURN YOUR FORM TO THE ABOVE ADDRESS.**			
1. REPORT DATE *(DD-MM-YYYY)* Sep 2015	**2. REPORT TYPE** Final		**3. DATES COVERED (From - To)** 2014–2015
4. TITLE AND SUBTITLE Large-Scale, Full-Wave Scattering Phenomenology Characterization of Realistic Trees: Preliminary Results			**5a. CONTRACT NUMBER** **5b. GRANT NUMBER** **5c. PROGRAM ELEMENT NUMBER**
6. AUTHOR(S) DaHan Liao and Traian Dogaru			**5d. PROJECT NUMBER** **5e. TASK NUMBER** **5f. WORK UNIT NUMBER**
7. PERFORMING ORGANIZATION NAME(S) AND ADDRESS(ES) US Army Research Laboratory ATTN: RDRL-SER-U 2800 Power Mill Road Adelphi, MD 20783-1148			**8. PERFORMING ORGANIZATION REPORT NUMBER** ARL-TR-7487
9. SPONSORING/MONITORING AGENCY NAME(S) AND ADDRESS(ES)			**10. SPONSOR/MONITOR'S ACRONYM(S)** **11. SPONSOR/MONITOR'S REPORT NUMBER(S)**
12. DISTRIBUTION/AVAILABILITY STATEMENT Approved for public release; distribution unlimited.			
13. SUPPLEMENTARY NOTES			
14. ABSTRACT Scattering characterization of realistic tree structures is performed to facilitate the development of low-frequency (P-band) foliage-penetration radars. The full-wave analysis approach employs a parallelized 3-dimensional finite-difference time-domain (FDTD) algorithm deployed on high performance computer systems to simulate the far-field electromagnetic responses of foliage scenes. The scattering behavior of a single tree is first considered as a function of frequency, polarization, signal incidence angle, and structural fidelity, and then large-scale simulations are carried out to examine the responses of a forest stand in both the frequency and imaging domains. The results featured are from the first phase of an ongoing study to investigate the feasibility of applying large-scale electromagnetic simulations to support airborne-based sensing of obscured ground targets.			
15. SUBJECT TERMS Electromagnetic scattering, foliage-penetration radar, full-wave simulation, radar imaging, tree scattering			

16. SECURITY CLASSIFICATION OF:			**17. LIMITATION OF ABSTRACT**	**18. NUMBER OF PAGES**	**19a. NAME OF RESPONSIBLE PERSON** DaHan Liao
a. REPORT Unclassified	**b. ABSTRACT** Unclassified	**c. THIS PAGE** Unclassified	UU	18	**19b. TELEPHONE NUMBER (Include area code)** (301) 394-1741

Standard Form 298 (Rev. 8/98)
Prescribed by ANSI Std. Z39.18

Contents

List of Figures

1. Introduction

Low-frequency airborne radar systems are a promising technology for the surveillance of foliage-obscured stationary and moving ground targets such as humans and vehicles.[1–4] Although much effort has been put forth in this area over the years, many unsolved problems remain as the foliage ecosystem itself—with scatterers of various shapes and sizes in multifarious arrangements—is inherently highly cluttered, and therefore, poses an intricate challenge for target detection and recognition, especially for a sensing platform in motion. Determination of target detectability ultimately necessitates a thorough fundamental understanding of the target and foliage scattering phenomenology (as well as the tree clutter statistics and attenuation) as a function of frequency, polarization, signal incidence angle, and foliage properties. As such, a full-wave electromagnetic solver is proposed in this study for scattering and propagation characterization in the foliage environment. Specifically, the analysis framework employs a parallelized finite-difference time-domain (FDTD) algorithm for deriving the far-field responses of complex realistic tree structures at P-band (200–500 MHz): the backscattering behavior of a single tree is first considered, and then large-scale simulations are performed to examine the responses of a forest stand in both the frequency and imaging domains. The solver is intended as a computational tool for evaluating the effectiveness of detection modes based on methods such as airborne synthetic aperture radar and ground moving target indication; nevertheless, the results and observations featured are also expected to be useful for remote sensing studies in which the primary interest lies in retrieving forest parameters from the scattering return.

2. Simulation Framework

As the first step, 3-dimensional representations of realistic tree structures need to be systematically constructed. The geometrical models in this work are created using the open-source random tree generator Arbaro,[5] which implements the rule-based growth algorithm developed by Weber and Penn.[6] Essentially, each tree structure is generated by following a series of recursive rules derived from geometrical observables. The tree structure in its entirety (trunk, multi-level branch complex, and leaves) can be exported from Arbaro in mesh form. Given the long wavelength at P-band, the effects of the leaves are often assumed to be negligible; therefore, only the trunk and branches are retained here for the electromagnetic simulations. Shown in Figs. 1–3 are some tree model examples.

Fig. 1 Quaking aspen (*Populus tremuloides*) tree model with increasing structural fidelity from left to right

Fig. 2 Sassafras tree model

Fig. 3 Eastern cottonwood (*Populus deltoides*) tree model

After the mesh has been properly processed (through operations such as closing of holes, translation and scaling, etc.), voxelization of the structure is performed with the parity count and ray stabbing methods.[7,8] The scattering responses of the resulting voxel grid are then calculated with a customized far-field FDTD algorithm.[9,10] The implemented code is fully parallelized and runs on large distributed computer systems using the message-passing interface (MPI) framework. In effect, the simulation domain is decomposed into rectangular sub-domains and the FDTD equations are solved separately for each sub-domain within one MPI process. The computational approach is highly scalable, even when the number of MPI processes is in the hundreds. More details on the electromagnetic solver can be found in our papers.[9,10]

3. Numerical Experiments

The backscattering return of a standalone tree above a half space is first analyzed. The tree species considered is the quaking aspen (*Populus tremuloides*), as shown in Fig. 1. Both the tree and the ground are assumed to be electrically homogeneous, with relative dielectric constant and conductivity (ε_r, σ_d) of (13.9, 39 mS/m) and (5.45, 20 mS/m), respectively. The tree has a height of 7.4 m, with a base diameter of 34 cm and a canopy diameter of 3.4 m. The co-polarized responses (radar cross section and phase difference) derived from simulating the structure with different levels of geometrical detail are displayed in Figs. 4–6, as a function of frequency and elevation incidence angle θ_i. The results are obtained by averaging the responses over 36 azimuth incidence angles ϕ_i. For the set of parameters employed here, it is seen that the backscattering mechanism of the trunk-ground dihedral provides the dominant signal response. The branch canopy has a tendency to enhance the radar cross section; this is more evident and consistent at horizontal-horizontal (*hh*) than at vertical-vertical (*vv*); the inclusion of the secondary branches in this case, however, does not significantly affect the overall return. Also note that the impact of the branch canopy seems to decrease as the incidence angle approaches grazing. In general, the *vv* responses on average are lower—and more sensitive to the incidence angle—than the *hh* responses; both of these observations can be attributed to the Brewster angle effect.

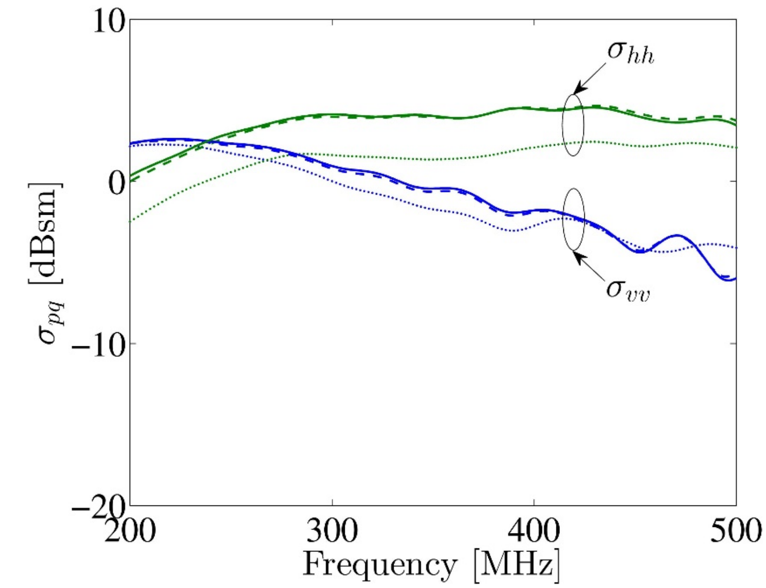

(a)

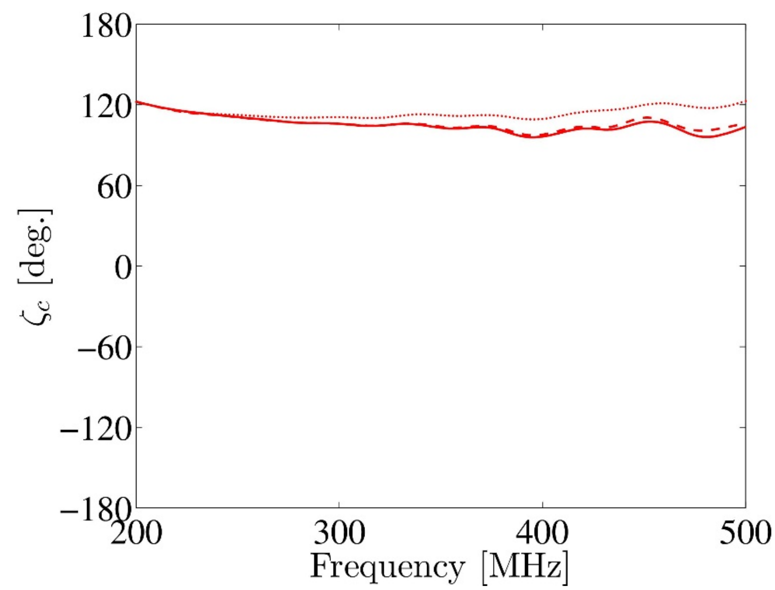

(b)

Fig. 4 Average response (co-polarized radar cross section and phase difference) of a single tree as a function of frequency and structural fidelity at $\theta_i = 45°$. Dotted line = trunk; dashed line = trunk + primary branches; solid line = trunk + primary and secondary branches.

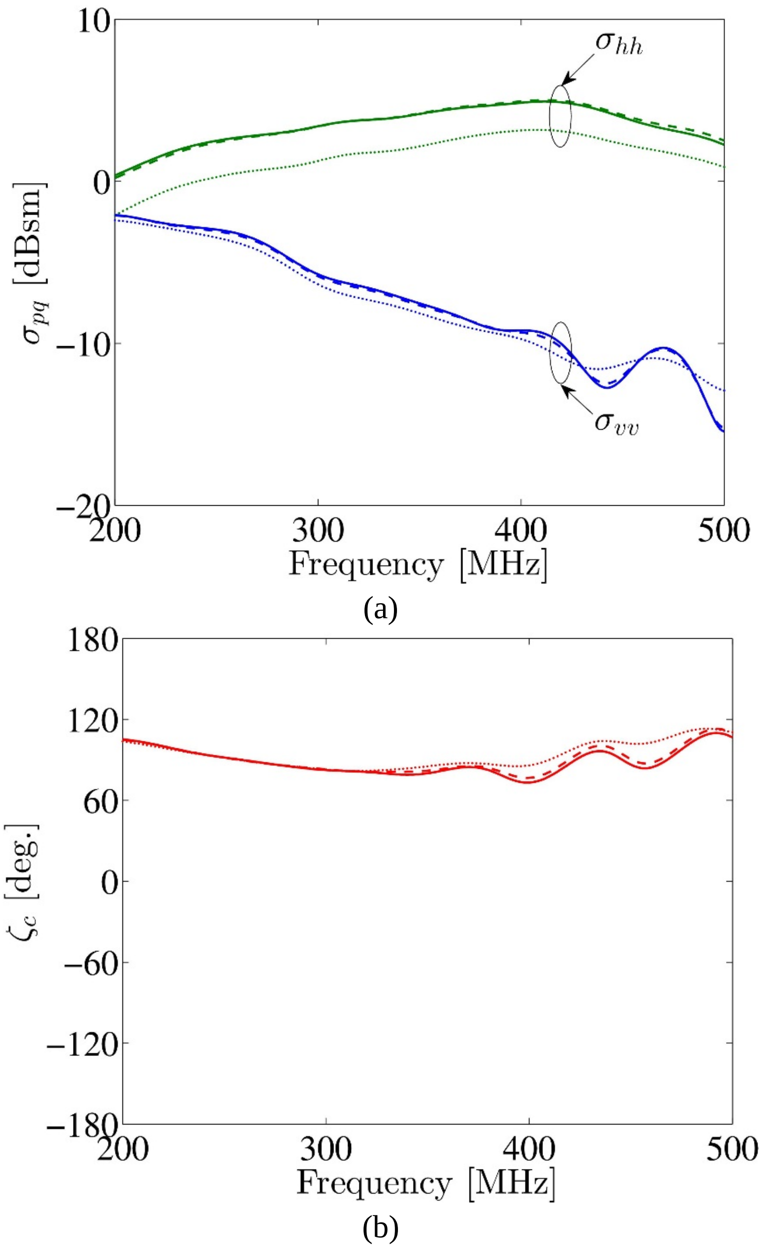

Fig. 5 Average response (co-polarized radar cross section and phase difference) of a single tree as a function of frequency and structural fidelity at $\theta_i = 60°$. Dotted line = trunk; dashed line = trunk + primary branches; solid line = trunk + primary and secondary branches.

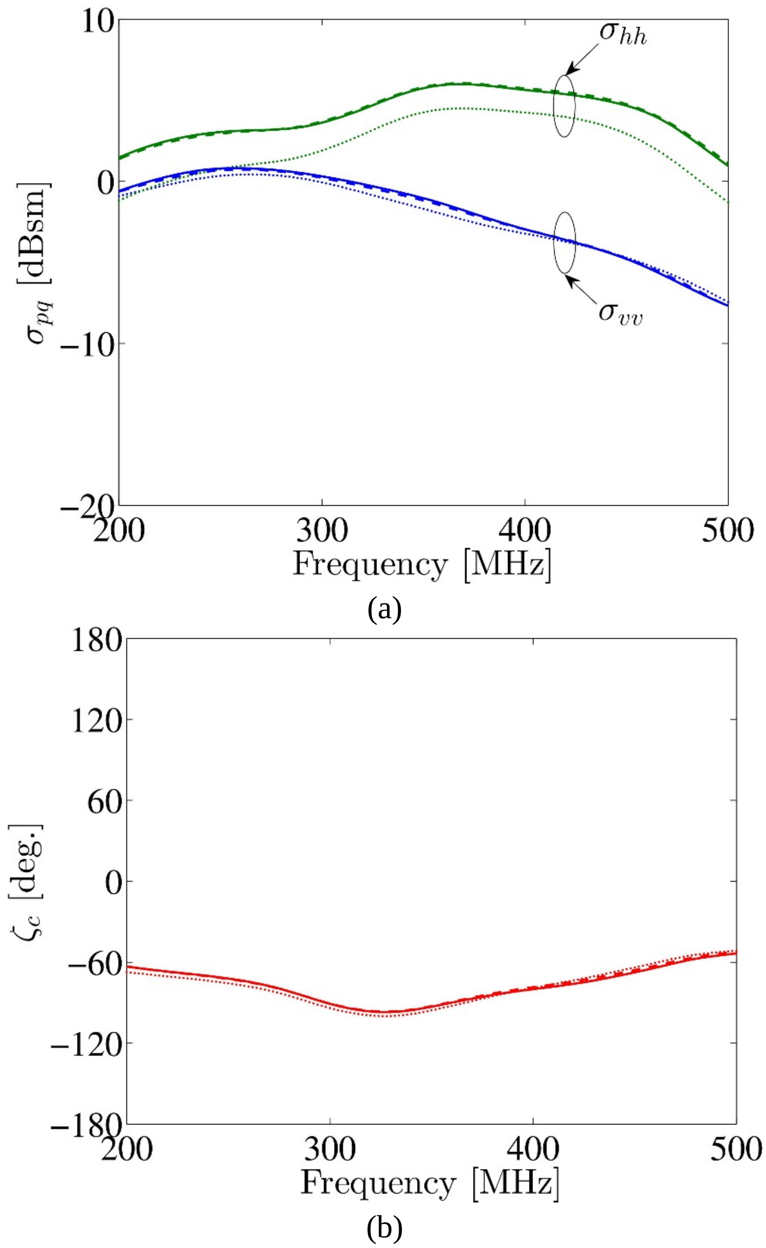

Fig. 6 Average response (co-polarized radar cross section and phase difference) of a single tree as a function of frequency and structural fidelity at $\theta_i = 75°$. Dotted line = trunk; dashed line = trunk + primary branches; solid line = trunk + primary and secondary branches.

Next, the simulation of a large forest scene consisting of 36 randomly generated trees is considered (Fig. 7). All the trees (with their full branch structures) are assumed to be of the same species as above, arranged within an approximately circular area. The dielectric properties are as previously described. The FDTD computational domain has dimensions 29 m × 29 m × 9 m and is discretized into 1.9 billion cells. Parallelized simulations were performed on a Cray XC30 system after partitioning the scene into 256 sub-domains. Each simulation run at 1 set of incidence angles required 413 CPU hours. The average response of the forest stand at $\theta_i = 75°$ is shown in Fig. 8. Imaging of the scene at each elevation incidence angle is demonstrated by re-focusing the backscattered fields captured over a 50° angular aperture (from $\phi_i = -25°$ to 25°, in 2.5° intervals). As seen in Fig. 9 ($\theta_i = 75°$), the locations of some of the tree trunks can be inferred from the co-polarized images. The images, however, are also populated with other clutter effects such as multipath interactions (i.e., coupling among trees) and speckle. The results at $\theta_i = 45°$ and $\theta_i = 60°$ are similar to those in Fig. 9.

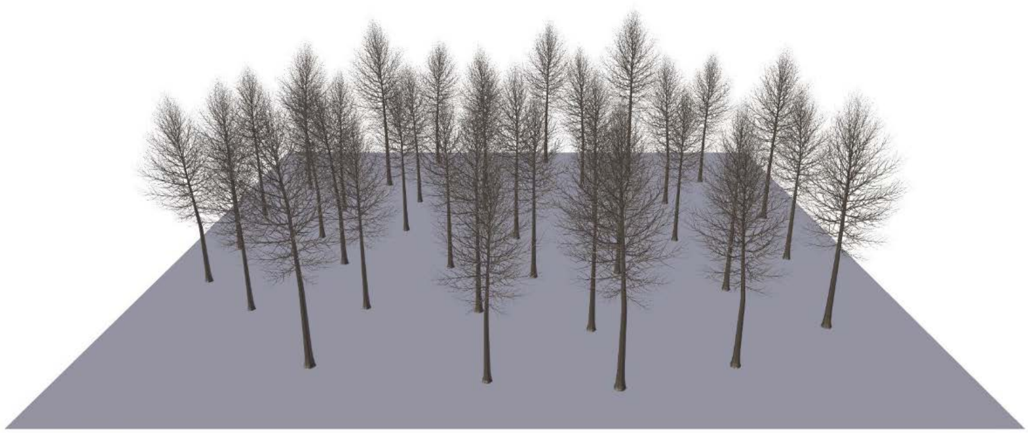

Fig. 7 Forest stand with 36 randomly generated trees. Average dimensions: tree height = 7.3 m; base diameter = 39 cm; canopy diameter = 3.2 m.

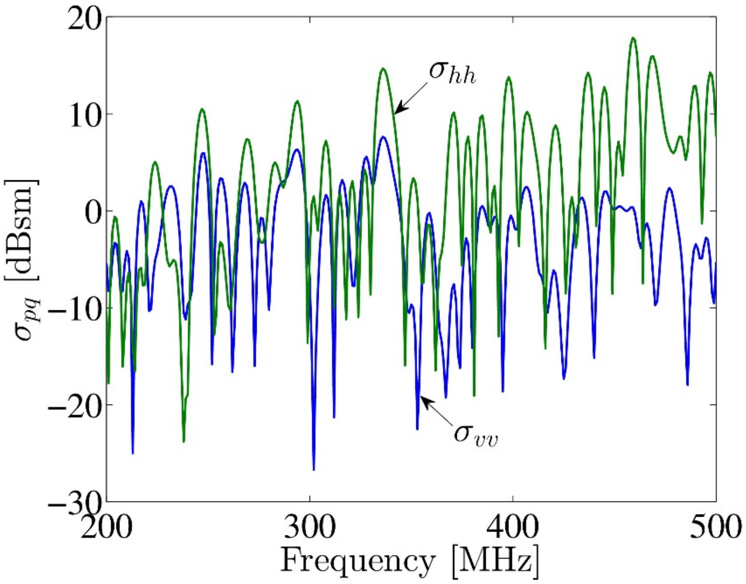

(a)

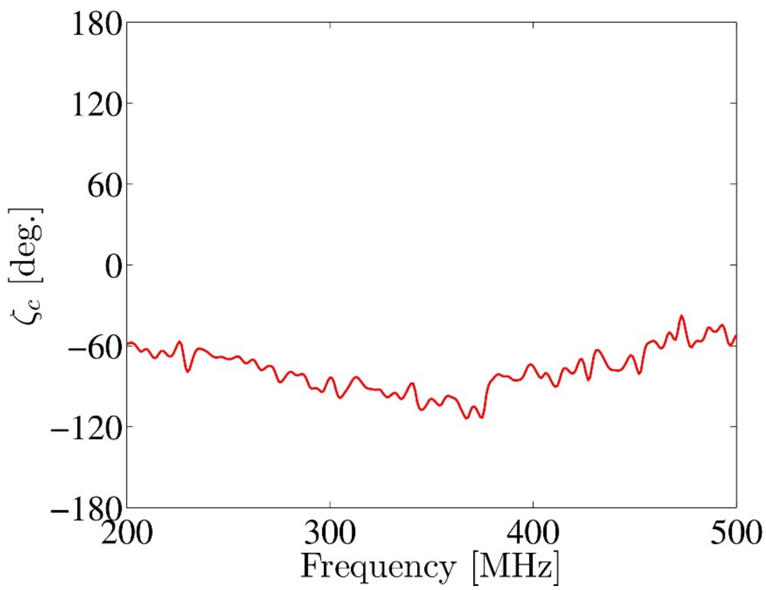

(b)

Fig. 8 Average response of scene in Fig. 7

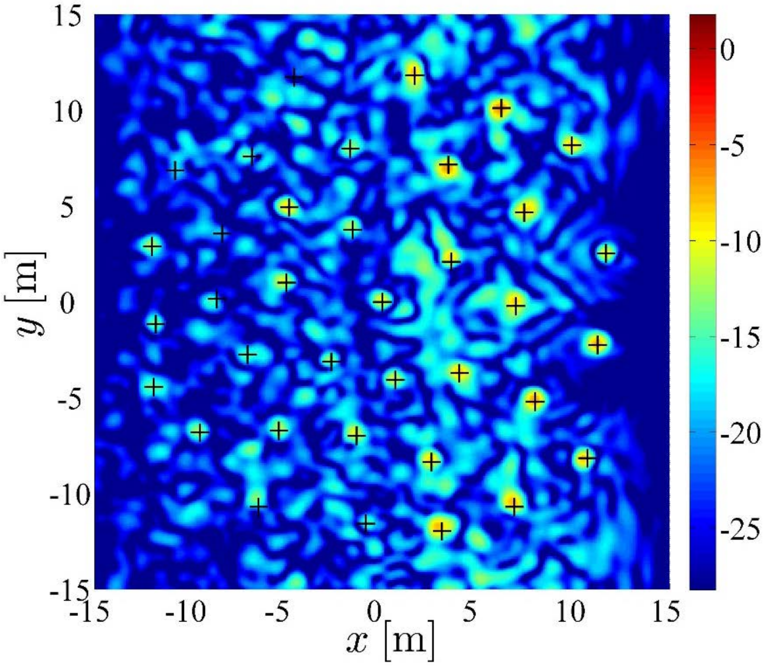

(a)

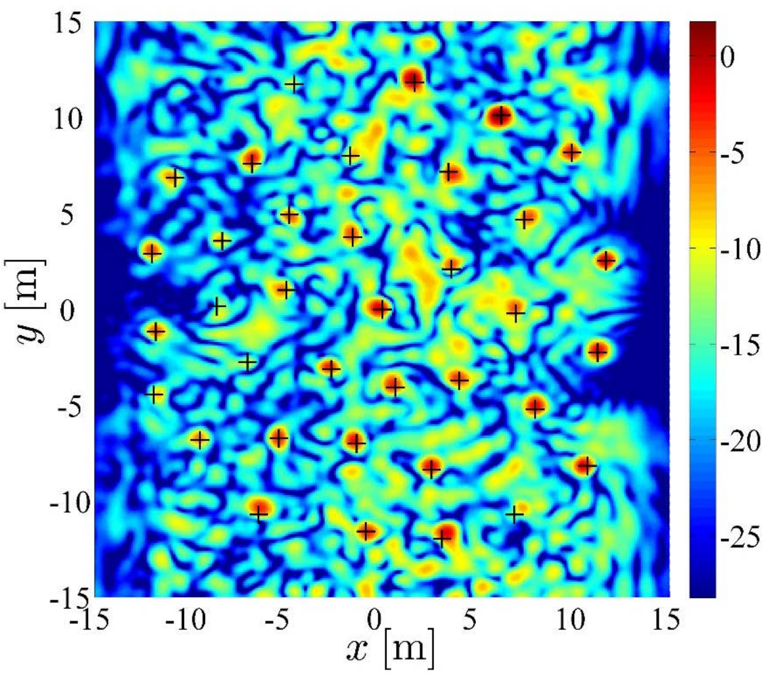

(b)

Fig. 9 Co-polarized images of scene in Fig. 7: a) *vv*; and b) *hh*

4. Conclusions

Full-wave simulations of scattering from trees are considered in this study. Geometrically realistic representations of tree structures are first created using an open-source random tree generator. Mesh processing and voxelization of the structures are then carried out to generate grid models that are amendable to numerical analysis. Finally, far-field electromagnetic scattering characterization is performed using a parallelized FDTD solver. To demonstrate the practicality of the analysis framework, the responses of a quaking aspen tree are investigated as a function of frequency, polarization, signal incidence angle, and structural fidelity. Subsequently, large-scale simulations are undertaken to examine the responses of a forest stand in both the frequency and imaging domains.

5. References

1. Colin E, Titin-Schnaider C, Tabbara W. FOPEN with polarimetric interferometry: validations with experimental data at P-band. Proceedings of the 2nd International Workshop on POLINSAR (ESA SP-586). 2005.
2. Allen MR, Jauregui JM, Hoff LE. FOPEN-SAR detection by direct use of simple scattering physics. Proceedings of 1995 Radar Conference. 1995.
3. Pastore L, Cantalloube H, Priou A, Dreuillet Ph. Evaluation of P-band foliage penetration through polarimetric high resolution SAR imaging with the RAMSES radar. Proceedings of 2002 Radar Conference. 2002.
4. Cantalloube H, Colin EK. POLINSAR for FOPEN using flashlight mode images along circular trajectories. Proceedings of 2007 Geoscience and Remote Sensing Symposium. 2007.
5. Diestel W. Arbaro—Tree generation for POV-Ray [accessed 2015]. http://arbaro.sourceforge.net.
6. Weber J, Penn J. Creation and rendering of realistic trees. Proc. Int. Conf. Comput. Graph. Interactive Tech., 1995.
7. Min P. Binvox—3D Mesh Voxelizer [accessed 2015]. http://cs.princeton.edu/~min/binvox.
8. Nooruddin FS, Turk G. Simplification and repair of polygonal models using volumetric techniques. IEEE Trans. Vis. and Comput. Graph. 2003.
9. Liao DH, Dogaru T. Full-wave characterization of rough terrain surface scattering for forward-looking radar applications. IEEE Trans. Antennas and Propagat. 2012.
10. Dogaru T, Le C. SAR images of rooms and buildings based on FDTD computer models. IEEE Trans. Geosci. and Remote Sens. 2009.

1 (PDF)	DEFENSE TECHNICAL INFORMATION CTR DTIC OCA
2 (PDF)	DIRECTOR US ARMY RESEARCH LAB RDRL CIO LL IMAL HRA MAIL & RECORDS MGMT
1 (PDF)	GOVT PRINTG OFC A MALHOTRA
5 (PDF)	DIRECTOR US ARMY RESEARCH LAB RDRL SER U C KENYON C LE D LIAO T DOGARU A SULLIVAN